EXPERIMENTAL AND NUMERICAL INVESTIGATION INTO DAMAGE MECHANISMS OF CFRP COMPOSITES UNDER OFF-AXIS COMPRESSION

Fan Yang[1] Yazhi Li[2] and Yan Li[3]

[1]School of Aeronautics, Northwestern Polytechnical University, Xi'an 710072, China
Email: tonyyoung789@mail.nwpu.edu.cn
[2] School of Aeronautics, Northwestern Polytechnical University, Xi'an 710072, China
Email: yazhi.li@nwpu.edu.cn
[3] School of Aeronautics, Northwestern Polytechnical University, Xi'an 710072, China
Email: liyan2016@mail.nwpu.edu.cn

Keywords: fiber reinforced polymer, off-axis compression, digital image correlation, plastic-damage model

Abstract
This paper presents an experimental investigation on the mechanisms of damage formation and evolution in unidirectional carbon fiber reinforced polymer composites subjected to off-axis compressive loading. A series of compressive tests were conducted on specimens with various off-axis angles. Different failure mechanisms as well as stress-strain responses were observed and studied. An elasto-plastic constitutive, consisting of an anisotropy yield surface, non-associative flow and a kinematic hardening rule, is proposed to characterize non-linear and inelastic behavior of unidirectional composites. Hydrostatic sensibility and coupling of complex stress state are taken into consideration. Combined with a series of physical-based failure criteria and associated damage evolution law, the constitutive model is implemented in Abaqus/Explict via user subroutine VUMAT. Comparison between the experimental and computational results indicates that the developed model is able to predict both the failure strength and the non-linear material response under combined loading.

1. Introduction

The increasing application of carbon fibre-reinforced polymer (CFRP) as primary structural parts in aviation and aerospace has drawn significant attention to the compressive failure of unidirectional laminates which is generally recognized as a combined result of various mechanisms. It is one of the most challenging task to comprehensively describe these behaviors. A considerable amount of research has been conducted in the past decades. Failure modes like matrix compression, fibre kinking and shear-driven have been experimentally observed and further explained in dozens of theoretical studies. Several recently proposed models [1,2] based on physical mechanisms successfully reflect different failure modes and correlate well with experimental phenomena.

Moreover, only successfully answering the question of when and how failures occur is not sufficient, as modern structural design concepts require an elaborate representation of the constitutive response. For a long time, CFRP is considered to be linear elastic until experimental evidences revealed the existence of its non-linearity. In addition, hydrostatic pressure has proved to be of influence on properties of polymers and polymer-matrix composites. In some investigations [3-5], non-linearity is expressed via empirical formula or spline interpolation in single direction, most of which are based on hyperelastic model, hence fail to describe unloading process and ingnore the interaction between

Excerpt from ISBN 978-3-00-053387-7

different stress components. Recently, some plastic constitutive models [6,7], which inherently account for unloading and coupling of multiple stress components, have been proposed for unidirectional composites. This seems to be a promising approach to solve all above problems.

The purpose of this paper is to study the compressive behavior of CFRP through the compression tests of off-axis specimens [8,9], which produce a set of combined stress states with uniaxial load and lead to different failure modes. To reproduce the experimental observations, a computational method is illustrated in the second part.

2. Experiments

2.1. Off-axis compression test

2.1.1. Specimens
Off-axis specimens were cut from a 16-ply CCF300/BA9916-II carbon/epoxy composite unidirectional laminate at different angles. In order to bring forth different failure modes and investigate their transition with each other, up to eight off-axis angles θ = 5°, 10°, 15°, 20°, 30°, 45°, 60°, 75° were selected, along with two special angles 0°(longitudinal compression) and 90°(transverse compression). To be sure about the repeatability, four specimens were prepared for each group. Nominal dimensions of the specimen are 14mm×7mm×2mm, which have an in-plane aspect ratio of 2 to avoid end effect. Parallelism tolerances of all opposing surfaces was strictly inspected, and the loading surfaces were well polished before the test. As smooth contact is essential to the free shear deformation induced by compression, contact surfaces of the loading ends were lubricated with a thin layer of MoS_2 lubricant.

2.1.2. Experimental procedures
The compression tests were carried out using an Instron 8872 machine with a 25kN load cell for specimens of off-axis angles less than 10° and a 5kN cell for the others. Each specimen was loaded at a stroke speed of 0.5mm/min. To ensure stable loading of small block specimens and eliminate potential bending, a special fixture was fabricated as shown in Fig.1. In addition, the fixture was settled between upper and lower compression platens which are self-adjusted parallel with each other via a pair of contact spherical surfaces underneath the lower platen. In-plane strain fields of the specimen were monitored and calculated by means of the digital image correlation (DIC) method. ARAMIS 4M is a non-contact optical system suitable for deformation measurements under quasi-static loads. In preparation for DIC measurement, the specimens were first painted white and then applied a stochastic spray pattern using black aerosol spray painting. A 70mm lens with distance ring was positioned at around 0.3m apart from specimen surface to capture speckle pattern images at a frequency of 1 frame per second. For the best strain computation, 12×12 pixel^2 facet size with a facet step of 10×10 pixel^2 was selected, and the computation size was 3×3 pixel^2.

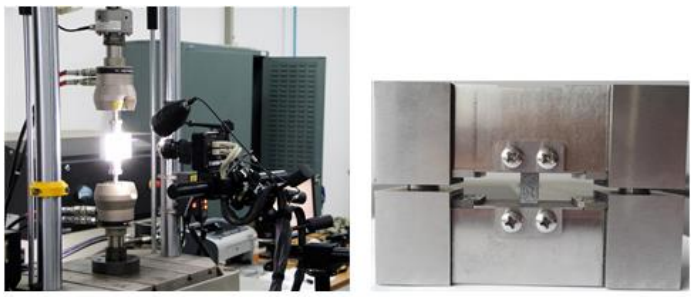

Figure 1. Off-axis compression test setup

Excerpt from ISBN 978-3-00-053387-7

2.1.3. Data processing

The axial stress was simply obtained from the applied load divided by the specimen cross-sectional area. Discrete strain data can be exported by the ARAMIS software, which was averaged to represent overall deformations of the specimen. Since DIC calculation may introduce larger error and inhomogeneity in the vicinity of specimen edges, a rectangular central area was selected for the strain evaluation.. Fig.2(b) illustrates that the choice of the area size has little effect on the measured strain, indicating good uniformity of deformation.

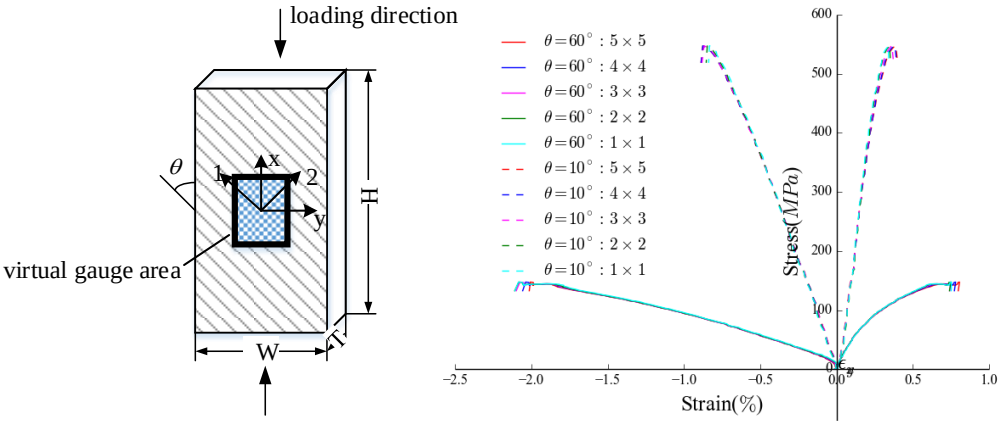

(a) off-axis specimen (b) size effect of virtual gauge area

Figure 2. Schematic of off-axis specimens

2.2. Experimental results

2.2.1. material response

Ttypical characteristics of stress-strain responses for different off-axis specimens are plotted in Fig.3(a). It can be seen that except for 0° and 5° off-axis specimens, all the other specimens undergo apparent non-linearity before failure. A short plateau can be witnessed in the stress-strain curve of some specimens, as obviously for 20°. A similar phenomenon has been mentioned by Koerber [9], indicating that the end surface friction is not adequately eliminated. Fortunately, this has little effect on ultimate strength and failure modes.

Fig.3(b) depicts the failure strengths of unidirectional composites under off-axis compression. The compressive strength of unidirectional composites reduces drastically as the off-axis angle varies from 0° to 45°, and then keeps steady with only a slight increase at 60°. It should be noticed that tests of 0° and 5° off-axis specimens should have underestimated the actual strengths. The irrational results are attributed to the premature end collapse, which will be discussed in the next section.

2.2.1. failure modes

Typical failure modes of the specimens are shown in Fig.4. Major damage modes happened in the middle region except for the kinking arose at both ends . For transverse compression ($\theta = 90^{\circ}$), specimens failed with either an oblique section or a wedge-like section shaped by double fracture facets. The fracture surface inclined around 60° with respect to the cross section. For large off-axis angles $\theta = 75^{\circ}, 60^{\circ}, 45^{\circ}, 30^{\circ}$, the sole matrix failure was witnessed with a fracture surface developed along the fibre direction. It is observed that the angle between the fracture surface and the through-thickness direction becomes smaller along with decreasing off-axis angle, which demonstrates a combination of in-plane shear with transverse compression.

Excerpt from ISBN 978-3-00-053387-7

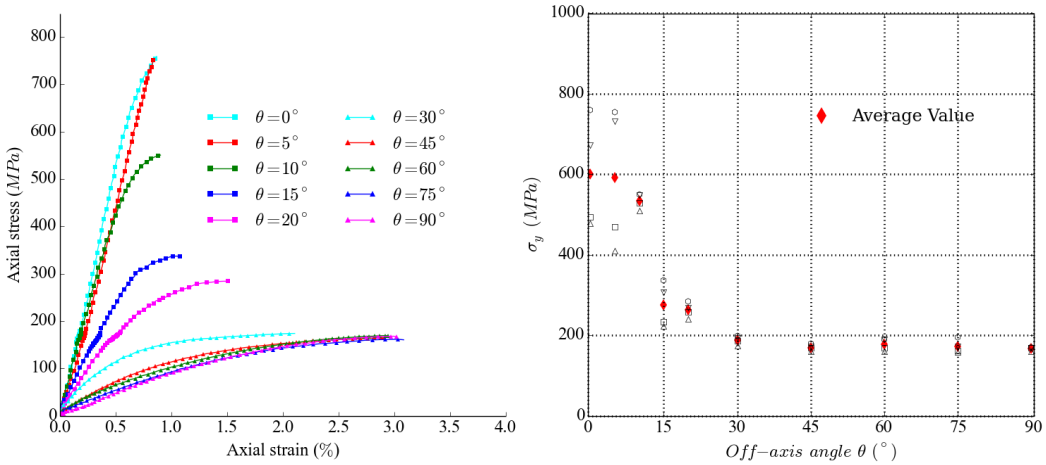

(a) stress-strain curve

(b) Failure strengths

Figure 3. Stress-strain curves of off-axis specimens under compression

In the cases of 15° and 20° off-axis angles, specimens fractured into several pieces along cracks parallel to the fibre. The fracture surface appeared to be scarcely slant, indicating an in-plane shear failure mode, also referred to as splitting in some literatures. A closer inspection of the fractured specimens with stereo microscope revealed that evident kink-bands have developed from the loading ends of 15° specimens. On the contrary, no sign of fibre kinking was found in 20° specimens. This observation suggests that the transition from splitting to kinking occurs between 15° to 20°. The fibre kinking failure mode became more dominated in specimens of 10° off-axis angle, where splitting can still be found, but did not tear the specimen apart.

Only two of the four 5° specimens achieved an intralaminar failure dominated by kinking. The other two, together with all the longitudinal compression ($\theta = 0^{\circ}$) specimens encountered end collapse with apparent delamination. It can be concluded that without extra measures to prevent end crush, the actual compressive strengths of low off-axis angle specimens are unlikely to be obtained using the current test method.

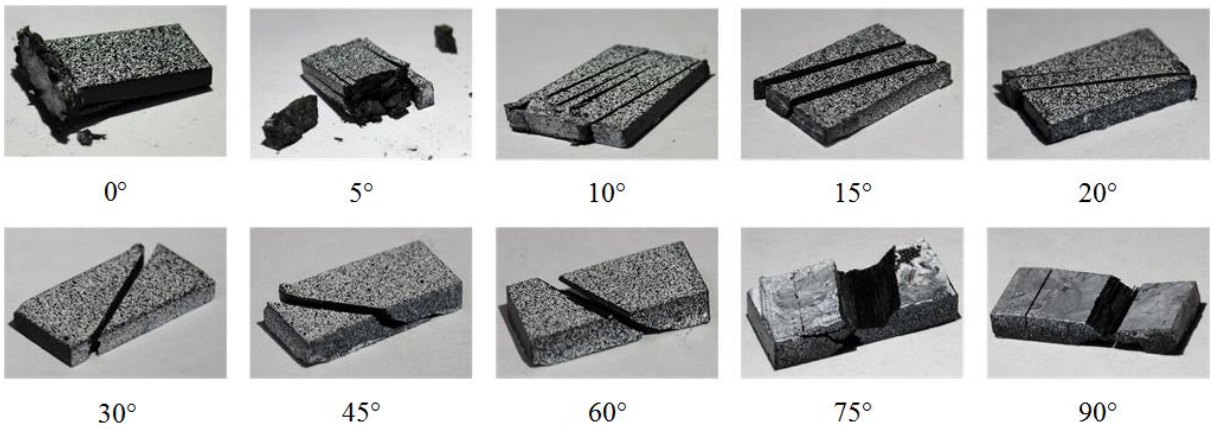

Figure 4. Failure modes of different specimens under compressive load

Excerpt from ISBN 978-3-00-053387-7

3. Plastic-damage model

3.1. Elasto-plastic constitutive for unidirectional laminate

3.1.1. yield function

Xie and Adams [6] proposed an approach to acquire yield criterion for unidirectional FRP by imposing $d\varepsilon_{11}^{p}=0$. Following their assumption, a series of yield criteria (eg. Vays [6]) have been readily obtained by removing all terms and brackets containing σ_{11} from isotropic criteria. However, for certain circumstances this assumption becomes more or less overly rigid. From the view point of micro-mechanics, the overall response of a composite can be deduced from individual behavior of its component materials and their geometrical arrangement. As the plastic behavior of polymer matrix is generally admitted, it is conceivable to predict the existence of plastic strain in longitudinal direction, even though it is always screened by the reinforcement phase a great more stiff and brittle.

More importantly, although plastic strain in fibre direction is negligible, longitudinal stress, on the contrary, has an effect on both yield strength and plastic flow. This effect may be amplified when the material is highly hydrostatic sensitive or combined stresses are applied just like the situations in the above experiment. Therefore, the authors prefer to reserve the effect of σ_{11}, whereras introduce a parameter χ to differentiate plastic behavior in fibre direction from the others. Base on the pressure dependent Raghava criterion [9], the yield surface is expressed as:

$$f=\sqrt{\frac{1}{6}\left[(\chi\sigma_{11}-\sigma_{22})^2+(\sigma_{22}-\sigma_{33})^2+(\sigma_{33}-\chi\sigma_{11})^2\right]+\sigma_{12}^2+\sigma_{23}^2+\sigma_{31}^2}-\mu p-\sigma_0=0 \tag{1}$$

where p is the redefined hydrostatic pressure:

$$p=-\left(\chi\sigma_{11}+\sigma_{22}+\sigma_{33}\right)/3 \tag{2}$$

The parameter χ can be deduced from a set of micro-mechanical formulae by imposing a rational assumption that only the longitudinal stress of matrix contribute to yielding. The rule of mixtures

$$E_{11}=E_f v_f+E_m v_m \tag{3}$$

$$1/E_{22}=v_f/E_f+v_m/E_m \tag{4}$$

along with the equal strains assumption in longitudinal direction, is adopted to determine the stress in matrix as:

$$\sigma_{11}^{m}=E_m\varepsilon_{11}=\frac{\sigma_{11}}{v_f E_f/E_m+v_m}=\chi\sigma_{11} \tag{5}$$

The in-situ values of fibre modulus E_f and matrix modulus E_m (both assumed to be isotropic) are always unavailable, but from Eq.3 and Eq.4 the ratio of them E_f/E_m can be solved. Only micro-mechanical parameters needed here are the volume fractions v_f and v_m which can be easily obtained through an inspection of the transverse cross-section.

3.1.2. flow rule

Once the yield criterion is fulfilled, the increment of plastic strain $d\varepsilon_p$ can be determined with the flow rule, reads:

$$d\boldsymbol{\varepsilon}_p=d\lambda\frac{\partial g}{\partial\boldsymbol{\sigma}} \tag{6}$$

Where $d\lambda$ is the plastic multiplier and g is the plastic potential function. According to the proposed yield criterion, a non-associative flow is given by Eq.7, where $f\neq g,\ \mu\neq\mu'$.

$$g=\sqrt{\frac{1}{6}\left[(\chi\sigma_{11}-\sigma_{22})^2+(\sigma_{22}-\sigma_{33})^2+(\sigma_{33}-\chi\sigma_{11})^2\right]+\sigma_{12}^2+\sigma_{23}^2+\sigma_{31}^2}-\mu' p \tag{7}$$

μ' is a material parameter to characterize the hydrostatic sensitivity of plastic flow. Dean and Crocker [10] elaborated three different ways to determine the value of μ'.

Excerpt from ISBN 978-3-00-053387-7

3.1.3. hardening law

The post-yield stress-strain behavior is taken into consideration via a non-linear kinemeatic hardening rule, which has been proved to be more suitable for polymer-matrix composites than isotropic expansion of the yield surface. The stress σ_{ij} in Eq.6 is substituted by $\xi_{ij}=\sigma_{ij}-\alpha_{ij}$, where α_{ij} denotes the back stress tensor. The increment of the back stress is given by Chun [11] as follow:

$$d\boldsymbol{\alpha}=\frac{c}{\sigma_0}(\boldsymbol{\sigma}-\boldsymbol{\alpha})d\varepsilon_e^p-\gamma\boldsymbol{\alpha}d\varepsilon_e^p \tag{8}$$

where c is a material constant and $d\varepsilon_e^p$ is the incremental effective plastic strain defined as:

$$d\varepsilon_e^p=\sqrt{\frac{2}{3}d\boldsymbol{\varepsilon}^P:d\boldsymbol{\varepsilon}^P} \tag{9}$$

The parameter γ is relevant to hydrostatic pressure and decreases in an exponential form with increasing value of the hydrostatic pressure *p*, reads:

$$\gamma=\gamma_0 e^{-\eta_\gamma p} \tag{10}$$

Given the consistency condition for kinematic hardening:

$$f_\sigma d\sigma+f_\alpha d\alpha=0 \tag{11}$$

the plastic multiplier dλ can be derived as:

$$d\lambda=\frac{f_\sigma \boldsymbol{C}d\varepsilon}{f_\sigma \boldsymbol{C}g_\sigma+\sqrt{\frac{2}{3}g_\sigma:g_\sigma}\,f_\alpha\left[\gamma\boldsymbol{\alpha}-\frac{c}{\sigma_0}(\boldsymbol{\sigma}-\boldsymbol{\alpha})\right]} \tag{12}$$

where $f_\sigma=\partial f/\partial\boldsymbol{\sigma}$, $f_\alpha=\partial f/\partial\boldsymbol{\alpha}$, $g_\sigma=dg/d\boldsymbol{\sigma}$ and $\boldsymbol{C}$ is the elastic stiffness tensor. In pure in-plane shear tests, the above model deduce to a linear relation between the logarithm of $d\sigma_{12}/d\varepsilon_{12}^p$ and ε_{12}^p. Parameter *c* and γ_0 can be determined from the curve fitting of test results.

3.2. Overview of the compressive failure criteria

According to Puck [12], the matrix-dominated failure is governed by the tractions τ_T, τ_L, σ_N, acting on the fracture plane, so that a modified Mohr-Coulomb criterion can be used to predict composite failure under transverse compression. Gutkin et al. [13] further improves this criterion to account for both matrix tension and compression failure in a same expression:

$$f_{\mathrm{m}}=\left(\frac{\tau_T}{S_T-\mu_T\sigma_N}\right)^2+\left(\frac{\tau_L}{S_L-\mu_L\sigma_N}\right)^2+\left(\frac{\langle\sigma_N\rangle}{Y_T}\right)^2 \tag{13}$$

where $\langle\bullet\rangle$ is the Macaulay bracket. S_T, S_L and Y_T denote transverse shear, longitudinal shear and transverse tensile strength respectively, and μ_T, μ_L are friction coefficients. Determination of these parameters is detailed in [14]. For 3D stress states, the fracture angles were obtained by trying serveral tentative values in the range $0\le\alpha\le\pi$, a numerical algorithm can be used to boost this process [15].

A three-dimensional stress based kinking model has been proposed by Pinho et al. [16] following Argon's approach which regards the formation of kink bands as a consequence of local microstructure collapse. Microcrack growth in the supporting matrix around deflected fibres is considered as a trigger. Hence, matrix failure criterion is applied in a misalignment coordinate that is obtained through two successive rotations of the original material coordinate. The same criterion is also used to predict failure of splitting, which happens when the longitudinal compression is not significant. Complete derivation of the kinking model can be found in [16].

Excerpt from ISBN 978-3-00-053387-7

4. Predictions

The proposed constitutive model, in combination with failure criteria outlined in the previous section, has been coded as a material subroutine in Abaqus/Explicit. The off-axis compression experiment is reproduced using a simple finite element model. The input data are listed in Table.1. The predicted stress-strain responses correlate well with experimental results in most cases (Fig.5). It is hard to tell weather the constitutive model accurately reflects the response of low off-axis angle specimens, because the experimental results are a little chaotic. However, from the predictions of 0° and 5°, it can be seen that the introducing of the plastic constitutive does not alert the fact that CFRP is linear elastic in the longitudinal direction.

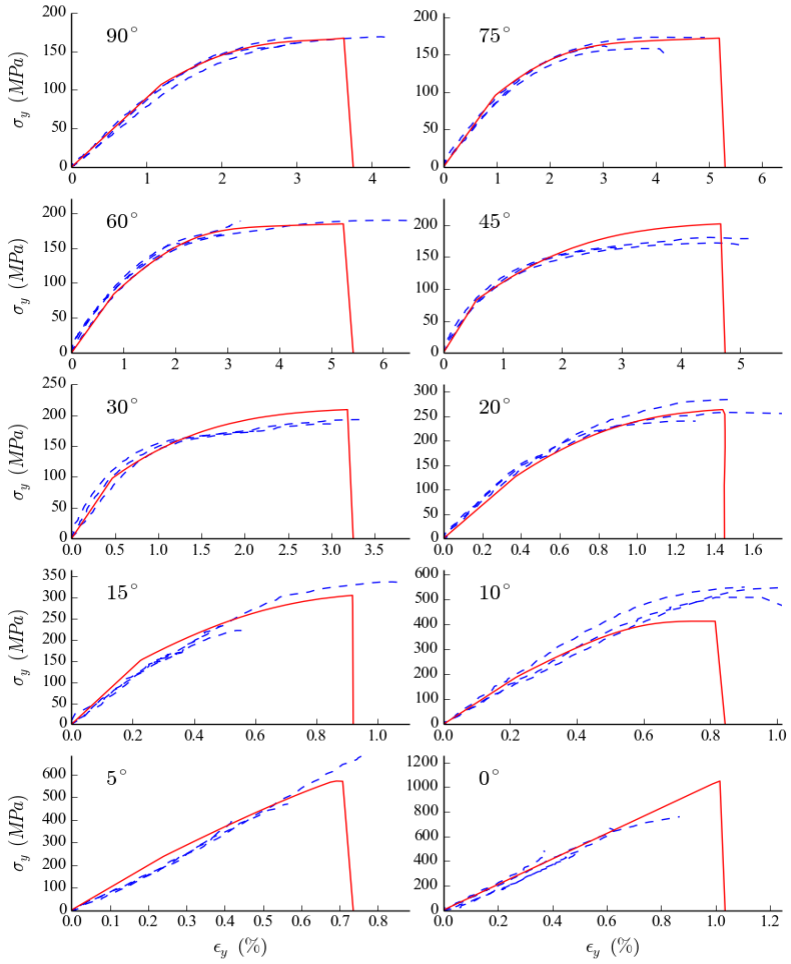

Figure 5. Predicted stress-strain response of unidirectional CFRP under off-axis compression

5. Conclusions

An experimental investigation of unidirectional CFRP composites under off-axis compression is presented. Fiber kinking can be observed at low off-axis angles, while matrix shear dominates the failure as the angle increases. To accurately reflect the non-linear stress-strain response under combined state of stress, a plastic model is introduced, consisting of a newly proposed yielding criterion, non-associated flow rule and a non-linear kinemeatic hardening. In combination with a set of failure criteria, the complete plastic model is implemented and used to reproduce the material responses of different off-axis compression specimens. The predictions correlate well with the experimental observations.

Excerpt from ISBN 978-3-00-053387-7

Table 1. Input data for prediction

[a] E_{11}	[a] E_{22}/E_{33}	[a] G_{12}/G_{13}	[a] G_{23}	[a] ν_{12}/ν_{13}	[a] ν_{23}	[a] X_T	[a] X_C	[a] Y_T
103790	8960	4700	3200	0.313	0.4	1805	1050	54
[a] Y_C	[a] S_L	[b] η_E	[b] η_G	[a] η_γ	[c] μ	[c] μ'	[c] γ_0	[c] c
167	96	0.18	0.18	0.002	1.17	1.57	75	3536

Note: [a]Basic material properties measured or computed from tests of the same material
[b]Effect of hydrostatic pressure on elastic modulus, obtained from [6]
[c]Paramters for plastic model acquired from transverse compression and V-notched shear tests

References

[1] A. Puck, J. Kopp, M. Knops. Guidelines for the determination of the parameters in Puck's action plane strength criterion. *Composites Science and Technology*, 62(3):371-378, 2002.
[2] Q. Bing, C.T. Sun. Specimen size effect in off-axis compression tests of fiber composites. *Composites Part B: Engineering*, 39(1):20-26, 2008.
[3] H.T. Hahn, S.W. Tsai. Nonlinear elastic behavior of unidirectional composite laminae. *Journal of Composite Materials*, 7(1):102-118, 1973.
[4] B.G. Falzon, P. Apruzzese. Numerical analysis of intralaminar failure mechanisms in composite structures. Part II: Applications. *Composite Structures*, 93(2):1047-1053, 2011.
[5] M. Xie, D.F. Adams. A plasticity model for unidirectional composite materials and its applications in modeling composites testing. *Composites science and technology*, 54(1):11-21, 1995.
[6] G.M. Vyas, S.T. Pinho, P. Robinson. Constitutive modelling of fibre-reinforced composites with unidirectional plies using a plasticity-based approach. *Composites Science and Technology*, 71(8):1068-1074, 2011.
[7] Q. Bing, C.T. Sun. Specimen size effect in off-axis compression tests of fiber composites. *Composites Part B: Engineering*, 39(1):20-26, 2008.
[8] H. Koerber, J. Xavier, P.P. Camanho. High strain rate characterisation of unidirectional carbon-epoxy IM7-8552 in transverse compression and in-plane shear using digital image correlation. *Mechanics of Materials*, 42(11):1004-1019, 2010.
[9] R.M. Caddell, R.S. Raghava, A.G. Atkins. A yield criterion for anisotropic and pressure dependent solids such as oriented polymers. *Journal of Materials Science*, 8(11):1641-1646, 1973.
[10] G.Dean, L. Crocker. Prediction of impact performance of plastics mouldings Part 1: Materials models and determination of properties. *Plastics, rubber and composites*, 36(1):1-13, 2007.
[11] B.K. Chun, H.Y. Kim, A. J Lee. Modeling the Bauschinger effect for sheet metals, part II: applications. *International Journal of Plasticity*, 18(5):597-616, 2002.
[12] A. Puck, H. Schürmann. Failure analysis of FRP laminates by means of physically based phenomenological models. *Composites Science and Technology*, 62(12):1633-1662, 2002
[13] G. Catalanotti, P.P. Camanho, A.T. Marques. Three-dimensional failure criteria for fiber-reinforced laminates. *Composite Structures*, 95:63-79, 2013.
[14] A. Puck., J. Kopp., M. Knops. Guidelines for the determination of the parameters in Puck's action plane strength criterion. Composites Science and Technology, 62(3), 371-378, 2002.
[15] J. Wiegand, N. Petrinic, B. Elliott. An algorithm for determination of the fracture angle for the three-dimensional Puck matrix failure criterion for UD composites. *Composites Science and Technology*, 68(12):2511-2517, 2008.
[16] S.T. Pinho, L. Iannucci, P. Robinson. Physically based failure models and criteria for laminated fibre-reinforced composites with emphasis on fibre kinking. Part II: FE implementation. Composites Part A: *Applied Science and Manufacturing*, 37(5):766-777, 2006.

Excerpt from ISBN 978-3-00-053387-7